2013

On the dose dependency of the bleachable and non-bleachable components of IRSL from K-feldspar: improved procedures for luminescence dating of Quaternary sediments

Bo Li
University of Wollongong, bli@uow.edu.au

Richard G. Roberts
University of Wollongong, rgrob@uow.edu.au

Zenobia Jacobs
University of Wollongong, zenobia@uow.edu.au

On the dose dependency of the bleachable and non-bleachable components of IRSL from K-feldspar: improved procedures for luminescence dating of Quaternary sediments

Abstract

The infrared (IR) stimulated luminescence (IRSL) and post-IR IRSL (pIRIR) signals from K-feldspar can, for convenience, be divided into two components, bleachable and 'non-bleachable', where the latter corresponds to the 'residual' signal observed in sunlight-bleached samples. In this paper, we examine the non-bleachable component of IRSL of K-feldspar for several sedimentary samples from across Eurasia. We observed a large variability in the residual doses among these samples after prolonged exposure to sunlight. By employing multiple elevated temperature (MET) IR stimulations at 50–300 °C, we show that the residual dose increases systematically with stimulation temperature, attaining values as high as ~50 Gy at 300 °C, even after several hours to tens of hours of exposure to unfiltered sunlight. We examined two samples in detail and found that the bleachable and non-bleachable components produced different dose response curves. Pulse annealing studies showed that the non-bleachable component is more stable than the bleachable component, suggesting that a preheat procedure cannot eliminate the non-bleachable component. Additional experiments revealed that the non-bleachable component is dose dependent. Owing to this dose dependency, we demonstrate mathematically and empirically that the simple subtraction of a residual dose from the measured equivalent dose (De) – which is the most common approach employed (if any residual dose is subtracted at all) – will result in underestimation of the actual De. We present a method to correct for the dose dependency of the residual dose, which can improve the accuracy of either MET-pIRIR or pIRIR age estimates for samples in which the non-bleachable component represents a significant fraction of the measured signals.

Disciplines

Medicine and Health Sciences | Social and Behavioral Sciences

On the dose dependency of the bleachable and non-bleachable components of IRSL from K-feldspar: improved procedures for luminescence dating of Quaternary sediments

Bo Li*, Richard G. Roberts, Zenobia Jacobs

Centre for Archaeological Science, School of Earth and Environmental Sciences, University of Wollongong, Wollongong, NSW 2522, Australia

*Corresponding author: bli@uow.edu.au

Abstract

The infrared (IR) stimulated luminescence (IRSL) and post-IR IRSL (pIRIR) signals from K-feldspar can, for convenience, be divided into two components, bleachable and 'non-bleachable', where the latter corresponds to the 'residual' signal observed in sunlight-bleached samples. In this paper, we examine the non-bleachable component of IRSL of K-feldspar for several sedimentary samples from across Eurasia. We observed a large variability in the residual doses among these samples after prolonged exposure to sunlight. By employing multiple elevated temperature (MET) infrared stimulations at 50°C to 300°C, we show that the residual dose increases systematically with stimulation temperature, attaining values as high as ~50 Gy at 300°C, even after several hours to tens of hours of exposure to unfiltered sunlight. We examined two samples in detail and found that the bleachable and non-bleachable components produced different dose response curves. Pulse-annealing studies showed that the non-bleachable component is more stable than the bleachable component, suggesting that a preheat procedure cannot eliminate the non-bleachable component. Additional experiments revealed that the non-bleachable component is dose dependent. Owing to this dose dependency, we demonstrate mathematically and empirically that the simple subtraction of a residual dose from the measured equivalent dose (D_e) – which is the most common approach employed (if any residual dose is subtracted at all) – will result in underestimation of the actual D_e. We present a method to correct for the dose dependency of the residual dose, which can improve the accuracy of either MET-pIRIR or pIRIR age estimates for samples in which the non-bleachable component represents a significant fraction of the measured signals.

Keywords: potassium feldspar, infrared stimulated luminescence, post-IR IRSL, MET-pIRIR, residual dose.

1. Introduction

Recent progress in understanding anomalous fading of the trapped charges related to the infrared stimulated luminescence (IRSL) signals in K-feldspar—that is, the leakage of electrons from traps at a much faster rate than would be expected from kinetic considerations—has raised the prospect of isolating a non-fading IRSL component for the dating of Quaternary deposits containing feldspars. By first bleaching feldspar grains using IR photons at 50°C and then measuring the post-IR IRSL (pIRIR) signal at an elevated temperature (>200°C), it is possible to preferentially sample traps that suffer least from fading (Thomsen et al., 2008; Buylaert et al., 2009; Thiel et al., 2011). Alternatively, the non-fading component can be identified by using a multiple elevated temperature (MET) stimulation procedure—the so-called MET-pIRIR protocol (Li and Li, 2011a, 2012a)—in which the feldspar grains are stimulated with IR at successively higher temperatures, from 50°C to 300°C.

Although the pIRIR signals measured at elevated temperature (e.g. >200 °C) have significantly reduced or negligible rates of fading compared to the IRSL signal measured at low temperatures (e.g., 50°C), they have also been found to be more difficult to bleach, requiring several hours of sunlight exposure to empty most of the light-sensitive traps (Thomsen et al., 2008; Li and Li, 2011a). At higher stimulation temperatures, the IRSL signal consists of components that are more resistant to bleaching (Li and Li, 2011a). In a study of several modern sand samples from Portugal, Denmark and India, Thomsen et al. (2008) measured residual doses of a few Gy in the pIRIR signal at 225°C [pIRIR(225)], while for modern aeolian sediments from China, Li and Li (2011a) measured residual doses of up to a few Gy in the MET-pIRIR signals at temperatures of 200°C and higher. These studies suggested that it may be necessary to consider the residual doses for relatively young samples only (e.g., D_e<100 Gy).

Significantly higher residual doses have subsequently been reported by others (e.g., Buylaert et al., 2011, 2012; Lowick et al., 2012). For example, Buylaert et al. (2011) reported residual doses of up

to ~20 Gy for the pIRIR 290°C signal [pIRIR(290)] from samples of modern Chinese loess, and Stevens et al. (2011) observed residual doses as high as ~40 Gy for loess samples from the southern Carpathian Basin. Lowick et al. (2012) reported highly variable residual doses in the pIRIR(290) signals, ranging up to ~150 Gy, and found that significantly large residual doses may be present when sunlight is attenuated by water. Sohbati et al. (2012) observed an increase in the pIRIR(225) residual doses with the D_e values of their samples. A similar observation was made by Buylaert et al. (2012) for the pIRIR(290) signals of 15 samples, and they suggested that the residual doses at the time of burial may be smaller than the residual doses inferred from laboratory measurements. Reimann and Tsukamoto (2012) found that the residual doses associated with the 50°C IRSL and pIRIR(150) signals were the same after a prolonged bleach, although the pIRIR signal is thought to be bleached more slowly than the 50°C IRSL signal.

In addition to the 'non-bleachable' component, the residual doses observed in the pIRIR signals are also partly induced by thermal transfer of charge from unstable, light-insensitive traps into the IRSL and pIRIR traps, due to the high preheat temperature (>300°C) employed in pIRIR protocols (Buylaert et al., 2012).

Given the observations of potentially substantial residual doses associated with the high-temperature pIRIR signals, whether measured at a single elevated temperature (such as 225°C or 290°C) or at multiple elevated temperatures (Thomsen et al., 2008; Li and Li, 2011a), the use of these pIRIR procedures for dating can only be safely applied to samples with a small composition of non-bleachable signals. In practice, researchers have estimated the residual doses from modern analogues or from artificially bleached samples, and these doses have been subtracted from the equivalent dose (D_e) measured using one of the pIRIR procedures (e.g., Buylaert et al., 2011; Li and Li, 2011a). There have been no systematic investigations yet, however, of the properties of the residual signal, nor of its effect on the accuracy of pIRIR age estimates. In this study, we study the properties of the non-bleachable IRSL component in samples from different regions of the world (China, France, Georgia, India and Oman) that have been deposited in a variety of natural settings. We show that the simple

subtraction of a residual dose (such as that obtained from a modern analogue) from the measured D_e can give rise to a significant underestimate in the size of the actual D_e, and the magnitude of this shortfall will be especially acute for young samples and for sediments that have a large residual dose at the time of deposition. We also propose a method of D_e determination that takes this residual dose into account.

2. Sample descriptions

Five sediment samples were examined in this study. To assess the variability in the properties of K-feldspars derived from different source rocks, we selected samples from different regions of Eurasia. The sample locations, expected ages and equivalent doses are summarised in Table 1. The samples have also been deposited in a variety of environmental settings at different times, from <1 to ~300 ka ago, and have a range of natural doses of between ~4.5 Gy and ~700-900 Gy. The Chinese loess sample (LC-004) consists of sediment grains that had been exposed to sunlight during aeolian transport before burial, while two of the samples consist of colluvial and alluvial sediments deposited at open-air archaeological sites in north-central India (Dhaba, DHB2-OSL4) and in the southern Caucasus, Georgia (Pinavera, PIN-OSL2). The remaining two samples were collected from a collapsed rock shelter in Oman (al-Hatab, ALH-1) and a collapsed cave in France (Les Cottés, LC10-07). Both of these are archaeological sites that have been dated using the optically stimulated luminescence (OSL) signal from quartz (R.G.R. and Z.J., unpublished data), as well as radiocarbon dating of bone at Les Cottés (Talamo et al., 2012).

3. Experimental procedures and analytical facilities

The samples were prepared for IRSL analysis using routine procedures (Aitken, 1998). First, they were treated with HCl acid and H_2O_2 solution to remove carbonates and organic matter, respectively, and then they were dried and sieved to obtain grains of 63–90, 90–125 and 125–180 μm in diameter (Table 1). The K-feldspar grains were separated from quartz and heavy minerals using a solution of sodium polytungstate with a density of 2.58 g/cm^3. The separated K-feldspar grains were

4

immersed in 10% HF acid for 40 min to etch the surfaces of the grains and remove the outer, alpha-irradiated portions, and then rinsed in HCl acid to remove any precipitated fluorides. The dried and etched K-feldspar grains were mounted as a monolayer on stainless steel discs of 9.8 mm diameter using "Silkospray" silicone oil as an adhesive. Grains covered the central ~5 mm diameter portion of each disc, corresponding to several hundred grains per aliquot.

IRSL measurements were made on an automated Risø TL-DA-20 reader equipped with IR diodes for stimulation (870 Δ 40 nm; Bøtter-Jensen et al., 2003). The total IR power delivered to the sample position was ~135 mW/cm^2 (Bøtter-Jensen et al., 2000), and laboratory irradiations were carried out on the reader using a calibrated ^{90}Sr/^{90}Y beta source. IRSL signals were detected by an Electron Tubes Ltd 9235B photomultiplier tube fitted with Schott BG-39 and Corning 7-59 filters to restrict transmission to 320–480 nm. Each aliquot was stimulated for 100 s, while being held at a chosen temperature of between 50°C and 300°C (see Table 2 for the stimulation temperatures used in the MET-pIRIR protocol) and the resulting signal was calculated as the sum of counts over the initial 10 s of each stimulation, with 'late light' subtraction (Aitken, 1998) of the background count rate over the final 10 s of each stimulation. We note that the IRSL intensity does not reach a constant level after 100 s of stimulation, but continues to decay, so the subtracted background consists of 'dark' counts intrinsic to the photomultiplier tube, scattered incident photons, and IRSL associated with the eviction of electrons from traps that are sensitive to IR radiation at the chosen stimulation temperature.

4. Results

4.1. Residual dose: variability between samples

To investigate whether or not samples from different geological settings have different residual doses associated with the MET-pIRIR signals, 4-6 aliquots of natural grains from each sample were exposed to unfiltered sunlight for 3–5 hr (in Wollongong during February and March 2012, between 10 a.m. and 4 p.m., with no cloud cover). We expected several hours of solar exposure to be sufficient to reduce the population of electrons in bleachable traps to a negligible level (Li and Li,

2011a). This was confirmed by bleaching samples ALH-1 and PIN-OSL2 for 3 days and samples DHB2-OSL4 and LC10-07 for one week, which resulted in a negligible further reduction in the residual doses compared to those measured after a 3–5 hr bleach. The following studies, therefore, are based on the residual doses measured by bleaching aliquots in sunlight for 3–5 hr.

After bleaching, we estimated the residual doses using the MET-pIRIR protocol of Li and Li (2012a), in which the signals induced by the regenerative and test doses are measured at stimulation temperatures of 50, 100, 150, 200, 250 and 300°C (Table 2). A preheat at 320°C for 60 s was applied to the regenerative and test doses to avoid significant influence from phosphorescence while recording the MET-pIRIR signal at 300°C. After IR stimulation of each test dose, a 'hot' IR bleach (100 s at 340°C) was adminstered to reduce the size of residual dose carried forward into the following regenerative dose cycle. At the start of each IRSL measurement, an 'IR-off' period of 10–50 s (see Table 2, footnote 'b') was applied to minimise the intensity of isothermal decay induced at elevated temperature. Fu et al. (2012) showed that, for some of their samples, there may be significant interference from thermoluminescence (TL) for the MET-pIRIR signal at high temperatures, even though the samples were preheated at a higher temperature than that used for IR stimulation. They observed that this may cause invalid D_e estimation and suggested that its effect should be monitored and minimised by holding the sample at the IR-measurement temperature for a period to decrease the size of the isothermal TL signal before IR stimulation. Typical IRSL and MET-pIRIR decay curves, including the signals observed during both the IR-off and IR-on periods, for sample LC10-07 are shown in Fig. 1. It can be seen that a longer IR-off period is needed for the signals measured at higher temperatures, and that the IR-off periods adopted in this study are sufficient to minimise the interference from isothermal TL.

The residual doses associated with the IRSL and MET-pIRIR signals after sunlight bleaching are shown in Fig. 2 for each sample. Considerable variation is evident in the residual doses among these samples and at the different IR stimulation temperatures. Sample ALH-1 has the smallest residual doses (ranging from a few Gy at 50°C to ~15 Gy at 300°C) and sample LC10-07 has the

largest (~55 Gy at 300°C). We note that no clear relation between the magnitude of the residual dose and the expected depositional age or D_e of the sample. For example, the two youngest samples (LC-004 and ALH-1) have the smallest residual doses, but the residual doses of the oldest sample (PIN-OSL2, ~200-300 ka) are bracketed by those of samples LC10-07 (~38 ka) and DHB2-OSL (~50 ka).

For all samples, the smallest residual doses (0–4 Gy) were obtained at an IR stimulation temperature of 50°C, and the size of the residual dose and the extent of variation (in Gy) both increase as the stimulation temperature is raised (Fig. 2). For the MET-pIRIR signal measured at 300°C, the residual doses range between ~10 and 55 Gy. Residual doses of this size may be small relative to the size of the D_e for some samples, such as PIN-OSL2, which has a residual dose of 39 Gy and a D_e of ~700-900 Gy. By contrast, the youngest sample, LC-004, has a residual dose of ~4 Gy when stimulated at 250°C, which is large (>60%) relative to the corresponding D_e value of ~6.5 Gy.

It is worth emphasising that a high residual dose of ~55 Gy was obtained for the MET-pIRIR(300) signal from sample LC10-07 (~38 ka), which corresponds to ~30% of the apparent D_e value (~147 Gy). This highlights the importance of obtaining accurate and precise constraints on the residual doses of all samples and not only those deposited recently, especially when stimulated at elevated temperatures. From these results and from those of other studies (e.g., Li and Li, 2011a; Buylaert et al., 2011; Stevens et al., 2011; Nian et al., 2012), it is clear that the residual dose associated with the non-bleachable component is highly variable from sample to sample, and that sunlight bleaching tests should be routinely conducted to estimate the likely minimum size of the residual dose at the time of sample deposition.

4.2. IRSL and pIRIR decay curves

Typical natural IRSL and MET-pIRIR signals for four samples (LC10-07, ALH-1, PIN-OSL2 and DHB2-OSL4) are shown in Fig. 3 as the measured 'Total' natural decay curves, together with the 'Residual' signals after sunlight bleaching measured from separate aliquots. We refer to the latter as the residual signals, associated with both the 'non-bleachable' traps and thermally transferred signals, and we do not distinguish between these two sources in the present study. All of the signals have been

7

normalised to the initial intensity of the natural IRSL signal measured at 50°C. These plots show that the proportional relationship between the IRSL and pIRIR signals varies significantly from sample to sample, and that the proportion of the residual signal relative to the natural signal also varies widely among these samples. To illustrate the latter, the ratios of the residual to total signals are plotted against stimulation time and temperature in Fig. 3e. For all four samples, the relative intensity of the residual signal increases, often substantially, with stimulation time at each temperature. As a consequence, MET-pIRIR signals measured at higher stimulation temperatures include a relatively larger contribution from the non-bleachable component, which accords with previous reports of elevated temperature pIRIR traps being harder to bleach than are IRSL traps at 50°C (Thomsen et al., 2008; Li and Li, 2011a).

4.3. IRSL and pIRIR dose response curves

Owing to the large size of the residual dose and signal intensity of sample LC10-07 (Fig. 3a), we used this sample for detailed study in the following experiments. To investigate the relation between the sizes of the residual signal and laboratory dose, we first heated 20 aliquots to 500°C, to empty the corresponding IR-sensitive traps, and then gave these aliquots a series of regenerative doses, followed by 4 hr exposure to sunlight to empty the bleachable traps. The remaining ('residual') IRSL and MET-pIRIR signals were then measured using the procedure in Table 2, and these data were used to construct sensitivity-corrected dose response curves (DRCs) of the residual signal as a function of regenerative dose (Fig. 4, filled squares). The residual signals show a clear dose dependency, and the rate of growth in signal with dose can be fitted using a single saturating exponential function. For comparison, the sensitivity-corrected 'total' IRSL and MET-pIRIR signals, which represent the sum of the bleachable and non-bleachable components and were obtained using the single-aliquot regenerative-dose (SAR) procedure in Table 2, are also shown in Fig. 4 (as open diamonds). The dose response of the 'bleachable' component was separated by subtracting the residual signal from the total signal, and the corresponding DRCs are shown by dashed lines in Fig. 4. On the basis of these data, it is evident that only a small fraction (~3% at 220 Gy) of the IRSL measured at 50°C consists of a non-

bleachable (residual) component, and that the proportion of this component increases with stimulation temperature, accounting for ~28% (at 220 Gy) of the total MET-pIRIR signal at 300°C.

To compare the shapes of the DRCs for the total, residual and bleachable signals measured at different stimulation temperatures, we normalised each set of curves to unity at a regenerative dose of 55 Gy (Fig. 5). For the total signals, the shapes of the DRCs differ according to stimulation temperature, with the 50°C IRSL dose response being similar to those of the MET-pIRIR signals at 100, 150 and 200°C, whereas the 250 and 300°C signals—the latter in particular—saturate at lower doses (Fig. 5a). By contrast, the residual signal DRCs display less variability in shape with stimulation temperature (Fig. 5c), so the bleachable signal DRCs follow a similar pattern to those for the total signal.

We calculated the characteristic saturation dose (D_0) values for the saturating exponential DRCs fitted to the total, residual and bleachable signals (shown as the lines of best fit in Fig. 4), as summarised in Table 3. Similar D_0 values were obtained for the total and bleachable signals. The D_0 values are highest for the total and bleachable IRSL signals measured at 50°C (420–450 Gy) and for the corresponding MET-pIRIR signals at 100, 150 and 200°C (350–600 Gy). At stimulation temperatures of 250°C and 300°C, the total and bleachable signals have D_0 values of ~300 Gy or less, which is consistent with previous findings for other samples (e.g., Li and Li, 2011a, 2012a). Compared to these signals, the residual signals of the sample LC10-07 have much lower D_0 values that span a narrower range (from ~160 to ~210 Gy) and are broadly consistent with each other at 2σ (Table 3). These results indicate that the same source traps are probably responsible for the residual signals measured at different stimulation temperatures, and that these traps differ from those associated with the bleachable component of the IRSL and pIRIR signals.

4.4. Thermal stability of the MET-pIRIR traps

We conducted a pulse annealing study to further test whether the non-bleachable traps responsible for the residual signals have a thermal stability similar to that of the bleachable traps. A fresh set of 11 aliquots of sample LC10-07 was heated to 500°C and each aliquot was then given a

regenerative dose of 330 Gy, after which they were bleached by sunlight for 4 hr and then preheated at 320°C for 60 s. The aliquots were then cut-heated to different temperatures ('annealed') between 300 and 500°C, before the IRSL and MET-pIRIR signals were measured using the procedure in Table 2 to obtain an estimate of L_x for each stimulation temperature. To monitor and correct for any sensitivity changes, each aliquot was then given a test dose (of 44 Gy) and the induced IRSL and MET-pIRIR signals were measured to estimate T_x for each stimulation temperature. Following these measurements, the aliquots were given another regenerative dose of 330 Gy and the above procedure was repeated, but without any exposure to sunlight, in order to study the thermal stability of the traps giving rise to the total signal.

Fig. 6a shows the sensitivity-corrected MET-pIRIR signals (L_x/T_x) measured at stimulation temperatures of 100, 150, 200, 250 and 300°C after each annealing; the L_x/T_x ratios plotted on the y-axis of Fig. 6 are normalised to a value of unity at an annealing temperature of 300°C. The pulse annealing curves for the IRSL signal measured at 50°C are not shown in Fig. 6 owing to the significant scatter in the data for the residual component, which is probably due to its low intensity (see Fig. 3a). For the MET-pIRIR signals, it is evident from Fig. 6a that the residual signals measured at higher temperatures are more thermally stable than those measured at lower temperatures: for example, the residual signal stimulated at 100°C starts to decrease from an annealing temperature of 350°C, whereas the 250 and 300°C residual signals are stable up to an annealing temperature of almost 400°C although the residual signal at 300°C appears to decrease at a slightly lower temperature than 200°C signal. A similar trend was observed by Li and Li (2011b) for the total MET-pIRIR signals of a sand dune sample from China, but the pulse annealing curves for the total MET-pIRIR signals from the same set of aliquots of sample LC10-07 exhibit a different pattern. As shown in Fig. 6b–f, the total MET-pIRIR signals (filled symbols and dashed lines) are stable up to an annealing temperature of nearly 350°C for all stimulation temperatures in the range 100–300°C, so the residual signals are systematically more thermally stable at the different stimulation temperatures. As the non-bleachable

component is more thermally stable than the bleachable component, it is not feasible to apply a preheat to preferentially remove the non-bleachable component and retain the bleachable component.

4.5. A correction method for residual doses

As indicated above, the residual dose can be responsible for a significant fraction of the total pIRIR signal measured, especially at the higher stimulation temperatures that are also the ones preferred for dating because of the greater thermal stability and lower fading rates of the associated traps. It is important, therefore, to be able to accurately correct for any residual dose when dating K-feldspar samples using pIRIR procedures, whether at a single elevated temperature or at multiple elevated temperatures.

In previous studies that have used high-temperature pIRIR signals for dating, estimates of the size of the residual dose have been made from measurements of modern analogues or samples of interest after artificial bleaching. The residual doses so obtained have then either been ignored (e.g., Thiel et al., 2011) or been subtracted from the measured D_e values of the samples of interest to calculate the D_e associated with the bleachable pIRIR traps (e.g., Li and Li, 2011a; Steven et al., 2011; Reimann et al., 2011; Lowick et al., 2012; Fu et al., 2012). This simple 'dose-subtraction' method is straightforward and might appear to be appropriate, but it will yield inaccurate D_e estimates for samples (such as LC10-07) with pIRIR signals that include a significant contribution from the non-bleachable component. This approach will, in principle, give an underestimate of the actual D_e, as can be demonstrated algebraically, as follows. If we assume that the actual D_e (i.e., the D_e associated with the bleachable traps) lies in the linear region of the dose response curve, then the measured D_e—which we refer to here as the 'apparent dose', D_a—is given as:

$$D_a = \frac{L_{BN} + L_{RN}}{L'_B + L'_R} D$$

where L_{BN} and L_{RN} denote the natural signal intensities of the bleachable and residual (i.e., non-bleachable) components, respectively, and L'_B and L'_R denote the corresponding intensities of the

bleachable and residual signals induced by regenerative dose D. Similarly, the residual dose (D_R) is given as:

$$D_R = \frac{L_{RN}}{L_B^\ell + L_R^\ell} D$$

The correct equation for determining the equivalent dose for the bleachable signal is:

$$D_e = \frac{L_{BN}}{L_B^\ell} D$$

But in the case of the simple dose-subtraction method, the corresponding quantity D_e' is calculated as:

$$D_e' = D_a - D_R = \left(\frac{L_{BN} + L_{RN}}{L_B^\ell + L_R^\ell} - \frac{L_{RN}}{L_B^\ell + L_R^\ell} \right) D = \frac{L_{BN}}{L_B^\ell + L_R^\ell} D$$

As a result, D_e' will be smaller than D_e, owing to the inclusion of L_R^ℓ in the denominator on the right-hand side. The extent of the underestimation will depend on the relative proportion of residual signal (L_R^ℓ) to bleachable signal (L_B^ℓ), with the magnitude of the shortfall increasing with L_R^ℓ. As the latter has been shown to increase with stimulation temperature in some samples of K-feldspar (e.g., all four samples in Fig. 3), it is important to take account of the effect of the residual signal in elevated-temperature pIRIR dating procedures.

To appropriately do so, we propose an 'intensity-subtraction' method instead of the dose-subtraction method. In the intensity-subtraction method, the total and residual signals are measured for the natural dose and each regenerative dose, and DRCs constructed for both signals. The method is illustrated in Fig. 7. Two groups of natural aliquots (Groups A and B) are prepared for each sample. Group A is used to measure the total signal of the natural aliquots (*N-total*), while the aliquots in Group B are bleached in sunlight for several hours before the residual signal is measured (*N-residual*).

Test doses are also given to both groups of aliquots, and the resulting MET-pIRIR signals measured using the procedure shown in Table 2. The aliquots in Group A are then given a series of regenerative and test doses, and the induced signals used to construct a sensitivity-corrected DRC for the total signal (*DRC-total*), again using the procedure in Table 2. Following these measurements, the same aliquots are given the same series of regenerative doses, after each of which the aliquots are bleached by sunlight for several hours before the residual signals are measured; a test dose is also applied at the end of each regenerative dose cycle, and the sensitivity-corrected data used to construct a DRC for the residual signal (*DRC-residual*).

The D_e value associated with the bleachable traps is then obtained by subtracting the pIRIR signal intensities for the *DRC-residual* from those of the *DRC-total* to derive the sensitivity-corrected DRC for the bleachable signal, on to which the sensitivity-corrected bleachable signal for the natural sample is projected to determine the D_e by interpolation; the latter signal is calculated by subtracting *N-residual* from *N-total*. This method is illustrated in Fig. 8, using the MET-pIRIR data obtained for LC10-07 at a stimulation temperature of 300°C. The bleachable component of the natural signal (filled triangle) has been estimated by subtracting *N-residual* (filled circle) from *N-total* (filled square), and the DRC of the bleachable traps (dashed line) has been calculated by subtracting *DRC-residual* (dotted line) from *DRC-total* (solid line). The D_e of ~130 Gy is then obtained by interpolating the filled triangle on to the dashed line. By contrast, the measured D_e (i.e., the D_e determined from *N-total* and *DRC-total*, equivalent to D_a in the notation above) is ~177 Gy, and an estimate of ~55 Gy for the residual dose can be obtained by projecting *N-residual* on to *DRC-total*. Subtracting this estimate of the residual dose from D_a, as in the dose-subtraction method, gives a D_e[4] value of ~122 Gy, which is

slightly smaller than the D_e value of ~130 Gy for the bleachable component calculated using the intensity-subtraction method.

In Fig. 8, the largest applied dose is 220 Gy. At such low doses, it might appear that the natural residual intensity (filled circle) is higher than the saturation intensity of the residual DRC (dotted line), whereas this is not so. Extending the fitted residual DRC to larger doses yields a

13

maximum residual signal intensity of 0.92 ± 0.02 at infinite dose. This value is entirely consistent with the natural residual intensity of 0.90 ± 0.05, which suggests that the natural residual signal is in, or is close to, saturation. This, in turn, supports the proposition that the residual signal is thermally and athermally stable (non-fading).

To further assess the extent of the differences between the estimates of D_e and D_e' with stimulation temperature, we have plotted the MET-pIRIR results for sample LC10-07 in Fig. 9. Fig. 9a shows the temperature dependence of the apparent doses associated with the total signal (i.e., D_a: filled squares) and the residual signal (i.e., D_R: open circles), and the corresponding D_e' values obtained for the bleachable signal (open squares) by subtracting the latter from the former using the simple dose-subtraction method. The smallest D_e' values were obtained from the IRSL signal measured at 50°C, with progressively larger values obtained at higher stimulation temperatures, culminating in the 300°C MET-pIRIR signal yielding a D_e' value of 130 ± 15 Gy (weighted mean and standard error for 6 aliquots). This dose-subtraction approach produces statistically consistent D_e' values for the MET-pIRIR signals at 200, 250 and 300°C, which could be interpreted as evidence that a stable (non-fading) and bleachable component had been measured. However, if these results are compared to those obtained using the intensity-subtraction method, it can be seen that the D_e' values are systematically smaller, by 7–12%, than the corresponding D_e determinations at IR stimulation temperatures of 50–300°C (Fig. 9b). A similar result was obtained when the two-step pIRIR(50, 290) procedure, in which the IRSL and pIRIR signals were measured at 50°C and 290°C, respectively (Thiel et al., 2011), was applied to sample LC10-07: the dose-subtraction D_e was ~13% lower than the intensity-subtraction D_e (Fig. 9b). These observed shortfalls for sample LC10-07 are consistent with the mathematical expectation that dose-subtraction estimates will underestimate the intensity-subtraction estimates.

We note that the D_e values obtained at high stimulation temperatures (>200°C) using both subtraction methods yield ages that are consistent at 2σ with the radiocarbon ages of ~38 cal. ka (Talamo et al., 2012) that bracket the layer of sample LC10-07. Thus, although the different approaches produce equally accurate ages for this particular sample, there are mathematical grounds to support the validity of the intensity-subtraction procedure for robust age estimation more generally.

To further test the accuracy of the alternative correction methods, a dose recovery test was conducted on sample DHB2-OSL4. Two groups of natural aliquots were first bleached by sunlight for 1 week. One group of aliquots was then given a laboratory dose of 55 Gy, which was subsequently measured using the MET-pIRIR protocol. The other group of aliquots was used measure the residual signals underlying the natural and regenerative doses, using the procedure outlined in Fig. 7. A total dose (D_a) of 72 ± 4 Gy was recovered for the MET-pIRIR (300°C) signal (Fig. 10a). If the residual dose (D_R) of 25 ± 3 Gy, obtained from the bleached aliquots, is subtracted from D_a, then the recovered dose associated with the bleachable signal (D_e) is calculated as 47 ± 5 Gy. This corresponds to a ratio of recovered to given dose of 0.85 ± 0.08, so the given dose is underestimated by ~15%. If the intensity-subtraction method is, instead, used to correct for the residual dose, a D_e value of 56 ± 3 Gy is obtained (Fig. 10a), which is in much closer agreement with the given dose of 55 Gy.

Fig. 10b shows the results of the dose recovery test for the MET-pIRIR signals of sample DHB2-OSL4 measured at different temperatures. The recovered/given dose ratios obtained using the dose-subtraction method are systematically smaller than unity at all temperatures, whereas the intensity-subtraction method yields ratios consistent with unity at temperatures of 150°C and above. The results for the two subtraction methods are, in general, most similar at lower stimulation temperatures; this pattern reflects the decreasing size of the residual (or non-bleachable) component relative to that of the bleachable component (Fig. 3d).

We conclude, therefore, that the dose-subtraction method should be used with caution, especially for samples in which the total pIRIR signal measured at temperatures of 200°C and above includes a relatively high proportion of the non-bleachable component, as may commonly be the case

with recently deposited sediments. However, we recommend that similar tests should be performed on more samples with independent age control, spanning a wide time interval, to check that the intensity-subtraction procedure is broadly applicable.

5. Implications for pIRIR dating of K-feldspars

The results presented above have a number of consequences for the accurate estimation of depositional ages for K-feldspars using elevated-temperature pIRIR signals.

First, based on the findings of previous studies and of this study, it has been shown that the relative proportion of bleachable and non-bleachable components is highly variable from site to site and from sample to sample (Fig. 2); it may also vary from grain to grain within any particular sample. Such variability precludes any simple generalisations about the likely significance of the non-bleachable signal in samples of K-feldspar, and we recommend that sunlight bleaching experiments be routinely conducted to establish the importance of the residual component for the samples of interest. If a significant non-bleachable component is found to be present, then a suitable method should be applied to correct for its influence on D_e and, hence, age estimation.

An alternative method to minimise the residual dose problem for young samples is to use a lower preheat temperature and pIRIR stimulation temperature (Madsen et al., 2011; Reimann et al., 2011, 2012), both of which should reduce the size of the residual dose. However, fading corrections are required at lower pIRIR stimulation temperatures (Reimann et al., 2011), and this involves additional uncertainties associated with fading rate measurements, as well as assumptions and limitations inherent to the fading correction model. The latter are especially problematic in the case of older samples, for which a fading correction procedure is not applicable.

Another important finding for the sample studied in detail in this paper is that the non-bleachable signal progressively increases in size at higher IR stimulation temperatures, and that it also increases relative to the size of the bleachable signal (Fig. 3a). This effect has the potential to lead to incorrect age estimation, and limits the value of the high-temperature pIRIR dating signals that appear to suffer

16

less from anomalous fading than the conventional IRSL signal measured at 50°C (Thomsen et al., 2008; Buylaert et al., 2009; Li and Li, 2011a). When choosing a suitable IR stimulation temperature using the pIRIR method, it is therefore necessary to consider not only the effects of anomalous fading, but also the possible existence of a significant non-bleachable component—especially for pIRIR signals stimulated at high temperature. The latter might be less prone to age shortfalls due to fading, but the existence of a significant residual dose at the time of deposition may give rise to D_e underestimates if the simple dose-subtraction method is used to account for it. On the other hand, if the sample had not been exposed to sufficient sunlight before burial to empty the bleachable traps and/or if no correction is made for the residual dose, then the use of pIRIR signals may give rise to D_e overestimates, rather than underestimates.

The calculated D_e ultimately depends on the relative importance of these competing influences, and an accurate estimate of the actual D_e will only be obtained using a pIRIR procedure if 3 conditions are met: (1) the bleachable component of the pIRIR signal was fully zeroed at the time of sample deposition; (2) the D_e associated with the bleachable traps that were filled and did not fade during the period of sample burial can be measured using one or more pIRIR signals; and (3) the residual dose associated with the non-bleachable pIRIR component can be estimated and subtracted correctly.

These conditions will not always be met, and the competing factors will not always be compensatory, so how can one validate the accuracy of D_e estimates? To reduce the extent of D_e underestimation associated with the residual dose, we recommend the use of the intensity-subtraction procedure to properly account for the non-bleachable pIRIR component. For an appropriate IR stimulation temperature, we would, in general, recommend the use of the MET-pIRIR procedure to identify the high-temperature region with a 'plateau' in D_e values, as this should include the most stable signals that are least affected by fading. However, as the non-bleachable component also increases in absolute and relative size with stimulation temperature, there may be advantages— particularly for young samples—in determining the D_e at lower stimulation temperatures, where the bleachable component accounts for a larger proportion of the total pIRIR signal.

Consequently, although the MET-pIRIR signals above 200°C are relatively immune to anomalous fading, these signals have relatively larger uncertainties associated with the correction for the non-bleachable component. For young samples, therefore, the effect of the residual dose may outweigh that of anomalous fading, so it might be preferable to determine the final ages from the MET-pIRIR signals stimulated at temperatures of no more than 200°C. By contrast, anomalous fading may be of primary concern for older samples, in which case the higher-temperature MET-pIRIR signals (e.g., at 250°C) would be more appropriate (Li and Li, 2012a, 2012b). For the latter samples, a plateau in the MET-pIRIR D_e/temperature or age/temperature plot could be used to identify the existence of a non-fading, bleachable component, and the D_e value at the low-temperature end of this plateau should have the highest ratio of bleachable to non-bleachable signal and, hence, yield the most accurate and precise estimate of age (e.g., Fig. 9b).

The use of the intensity-subtraction method to account for the non-bleachable pIRIR component suffers from the same drawback as the dose-subtraction method: namely, at least two sets of aliquots are required to determine the D_e of each sample (Fig. 7). One set is used to measure the natural signal intensity and regenerative dose intensities for the total and non-bleachable signals (Group A), while the other set is needed to estimate the residual intensity of the natural signal, following exposure to sunlight (Group B). This approach requires that both groups of aliquots consist of grains that were bleached to the same extent at the time of deposition, and that both respond similarly to the laboratory treatments. This degree of homogeneity may be reasonable to assume in some cases, such as aliquots composed of hundreds or thousands of grains that had been fully bleached in antiquity, but the residual dose may vary greatly from grain to grain in partially bleached samples, which would invalidate the use of a dual-aliquot correction procedure—whether it be based on the dose-subtraction or intensity-subtraction method. Sunlight bleaching experiments are not able to establish the residual intensity of the natural signal for those grains that had been bleached most completely at the time of deposition without some independent means of identifying the latter. Studies of the non-bleachable component among individual grains of K-feldspar would, therefore, be a useful first step to determining its range

of variability at the single-grain level, and discern any patterns that could be used to recognise the most fully bleached grains in a heterogeneously bleached population.

6. Conclusions

Given our present state of knowledge about the size of the non-bleachable component in different samples of K-feldspar, both in absolute terms and relative to the size of the sample D_e, it is premature to expect that accurate ages can be obtained routinely for recently deposited and/or partially bleached sediments using elevated-temperature pIRIR signals. Although the latter are less prone to fading than the conventional IRSL signal measured at 50°C, they are accompanied by much higher residual doses, which can greatly exceed the D_e values of young samples, in particular. For partially bleached samples of any age, it is not clear how to determine the appropriate residual dose for the grains that were bleached most completely at the time of deposition. In the case of fully bleached samples, the residual dose can be estimated using an intensity-subtraction method, which we have shown mathematically is more appropriate than simply subtracting either the dose remaining after bleaching the sample in sunlight or the dose measured in a modern analogue. The latter, dose-subtraction, method is apt to yield D_e underestimates, as we have demonstrated experimentally using a dose recovery test.

To maximise the benefits gained by preferentially stimulating the electron traps that are least prone to anomalous fading, future research could usefully focus on documenting the variability in the non-bleachable component of elevated-temperature pIRIR signals among individual grains of the same sample and of different samples. To obtain accurate pIRIR ages routinely will require an improved understanding of the extent and cause of variation in residual doses within and between samples. Incorporation of this knowledge into pIRIR dating procedures may make it feasible to determine reliable ages from the D_e values and residual doses estimated for individual aliquots and grains.

References

Bøtter-Jensen, L., Andersen, C.E., Duller, G.A.T., Murray, A.S., 2003. Developments in radiation, stimulation and observation facilities in luminescence measurements. Radiation Measurements 37, 535-541.

Bøtter-Jensen, L., Bulur, E., Duller, G.A.T., Murray, A.S., 2000. Advances in luminescence instrument systems. Radiation Measurements 32, 523-528.

Buylaert, J.P., Murray, A.S., Thomsen, K.J., Jain, M., 2009. Testing the potential of an elevated temperature IRSL signal from K-feldspar. Radiation Measurements 44, 560-565.

Buylaert, J. P., Thiel, C., Murray, A. S., Vandenberghe, D. A. G., Yi, S., Lu, H., 2011. IRSL and post-IR IRSL residual doses recorded in modern dust samples from the Chinese Loess Plateau. Geochronometria 38, 432–440.

Buylaert, J.P., Jain, M., Murray, A.S., Thomsen, K.J., Thiel, C., Sohbati, R., 2012. A robust method for increasing the age range of feldspar IRSL dating. Boreas, DOI: 10.1111/j.1502-3885.2012.00248.x

Fu, X., Li, B., Li, S.H., 2012. Testing a multi-step post-IR IRSL dating method using polymineral fine grains from Chinese loess. Quaternary Geochronology, in press.

Li, B., Li, S.H., 2011a. Luminescence dating of K-feldspar from sediments: A protocol without anomalous fading correction. Quaternary Geochronology 6, 468-479.

Li, B., Li, S.H. 2011b. Thermal stability of infrared stimulated luminescence of sedimentary K-feldspar. Radiation Measurements 46, 29-36.

Li, B., Li, S.H., 2012a. Luminescence dating of Chinese Loess beyond 130 ka using the non-fading signal from K-feldspar. Quaternary Geochronology, in press.

Li, B. Li, S.H., 2012b. A reply to the comments by Thomsen et al. on "Luminescence dating of K-feldspar from sediments: A protocol without anomalous fading correction". Quaternary Geochronology 8: 49-51.

Lowick, S.E., Trauerstein, M., Preusser, F., 2012. Testing the application of post IR-IRSL dating to fine grain waterlain sediments. Quaternary Geochronology 8, 33-40.

Madsen, A.T., Buylaert, J.P., Murray, A.S., 2011. Luminescence Dating of Young Coastal Deposits from New Zealand Using Feldspar. Geochronometria 38, 379-390.

Nian, X.M., Bailey, R.M., Zhou, L.P., 2012. Investigations of the post-IR IRSL protocol applied to single K-feldspar grains from fluvial sediment samples. Radiation Measurements, in press.

Reimann, T., Thomsen, K.J., Jain, M., Murray, A.S., Frechen, M., 2012. Single-grain dating of young sediments using the pIRIR signal from feldspar. Quaternary Geochronology 11, 28-41.

Reimann, T., Tsukamoto, S., 2012. Dating the recent past (< 500 years) by post-IR IRSL feldspar - Examples from the North Sea and Baltic Sea coast. Quaternary Geochronology 10, 180-187.

Reimann, T., Tsukamoto, S., Naumann, M., Frechen, M., 2011. The potential of using K-rich feldspars for optical dating of young coastal sediments - A test case from Darss-Zingst peninsula (southern Baltic Sea coast). Quaternary Geochronology 6, 207-222.

Sohbati, R., Murray, A.S., Buylaert, J.P., Ortuno, M., Cunha, P.P., Masana, E., 2012. Luminescence dating of Pleistocene alluvial sediments affected by the Alhama de Murcia fault (eastern Betics, Spain) - a comparison between OSL, IRSL and post-IR IRSL ages. Boreas 41, 250-262.

Stevens, T., Markovic, S.B., Zech, M., Hambach, U., Sumegi, P., 2011. Dust deposition and climate in the Carpathian Basin over an independently dated last glacial–interglacial cycle. Quaternary Science Reviews 30, 662-681.

Talamo, S., Soressi, M., Roussel, M., Richards, M., Hublin, J., 2012. A radiocarbon chronology for the complete Middle to Upper Palaeolithic transitional sequence of Les Cottés (France). Journal of Archaeological Science 39, 175-183.

Thiel, C., Buylaert, J.P., Murray, A.S., Terhorst, B., Hofer, I., Tsukamoto, S., Frechen, M., 2011. Luminescence dating of the Stratzing loess profile (Austria) - testing the potential of an elevated temperature post-IR IRSL protocol. Quaternary International 234, 23-31.

Thomsen, K.J., Murray, A.S., Jain, M., Bøtter-Jensen, L., 2008. Laboratory fading rates of various luminescence signals from feldspar-rich sediment extracts. Radiation Measurements 43, 1474-1486.

Figure captions

Figure 1: Typical IRSL and MET-pIRIR signals from sample LC10-07 measured at different stimulation temperatures. The shaded area shows the signal observed in the 'IR-off' period.

Figure 2: The residual doses obtained after sunlight bleaching of different samples, plotted against the MET-pIRIR stimulation temperature. The data for the Chinese loess sample (LC-004) are from Fu et al. (2012). All data points are based on the average of four aliquots. The legend includes the approximate measured or expected D_e value and depositional age of each sample.

Figure 3: Comparison of the natural (solid lines) and residual (dashed) IRSL and MET-pIRIR signals obtained from samples (a) LC10-07, (b) ALH-1, (c) PIN-OSL2 and (d) DHB2-OSL4 at different stimulation temperatures (shown below the curves). All IRSL curves are normalised to the initial intensity of the natural 50°C IRSL signal (stimulation time at t = 0 s). The total and residual signals are each based on one separate aliquot. (e) Ratios of residual/total signal intensities as a function of stimulation time and temperature (shown at the top of the plot) for each of these samples.

Figure 4: Dose response curves (DRCs) for the total, residual and bleachable MET-pIRIR signals at different stimulation temperatures. The residual DRCs (red solid lines) were obtained using aliquots bleached by sunlight for 4 hr. The DRCs of the bleachable signals (dashed lines) were obtained by subtracting the residual DRCs from the total DRCs (black solid lines).

Figure 5: Comparison of the dose response curves from the (a) total signals, (b) bleachable signals and (c) residual signals for the IRSL and MET-pIRIR signals measured at different stimulation temperatures. All DRCs are normalised to unity at 55 Gy.

Figure 6: (a) Pulse annealing results for the residual IRSL and MET-pIRIR signals measured at different stimulation temperatures. (b) to (f) Pulse annealing curves for the residual and total signals measured at 100, 150, 200, 250 and 300°C, respectively. All curves are normalised to the initial value (i.e., at an annealing temperature of 300°C).

22

Figure 7: Procedure to determine the bleachable signal DRC and the natural total and residual signal intensities using the 'intensity-subtraction' method.

Figure 8: An example of the 'intensity-subtraction' method based on the results of the 300°C MET-pIRIR signals from sample LC10-07. The natural bleachable signal (N-bleachable, filled triangle) is estimated by subtracting the natural residual signal (N-residual, filled circle) from the natural total signal (N-total, filled square). The DRC of the bleachable signal (dashed line) is obtained by subtracting the DRC of the residual signal (dotted line) from that of the total signal (solid line). D_a is the apparent dose obtained from the total signal, and D_e is the equivalent dose of the bleachable signal.

Figure 9: (a) The MET-pIRIR equivalent doses for sample LC10-07 obtained from the total (D_a), residual (D_R) and bleachable (D_a-D_R) signals using the 'dose-subtraction' method, plotted against IR stimulation temperature. (b) Comparison of results obtained for sample LC10-07 using the 'dose-subtraction' and 'intensity-subtraction' methods. The filled and open squares represent the results of the MET-pIRIR procedure. The filled and open diamonds are the results of the two-step pIRIR(50, 290) procedure (Thiel et al., 2011), in which the IRSL and pIRIR signals were measured at 50°C and 290°C, respectively.

Fig. 10: (a) N-total, N-residual and N-bleachable intensities and DRCs for the 300°C MET-pIRIR signals measured during a dose recovery test on sample DHB2-OSL4. Symbols and abbreviations are the same as in Fig. 8. (b) Comparison of dose recovery ratios obtained for sample DHB2-OSL4 using the 'dose-subtraction' and 'intensity-subtraction' methods.
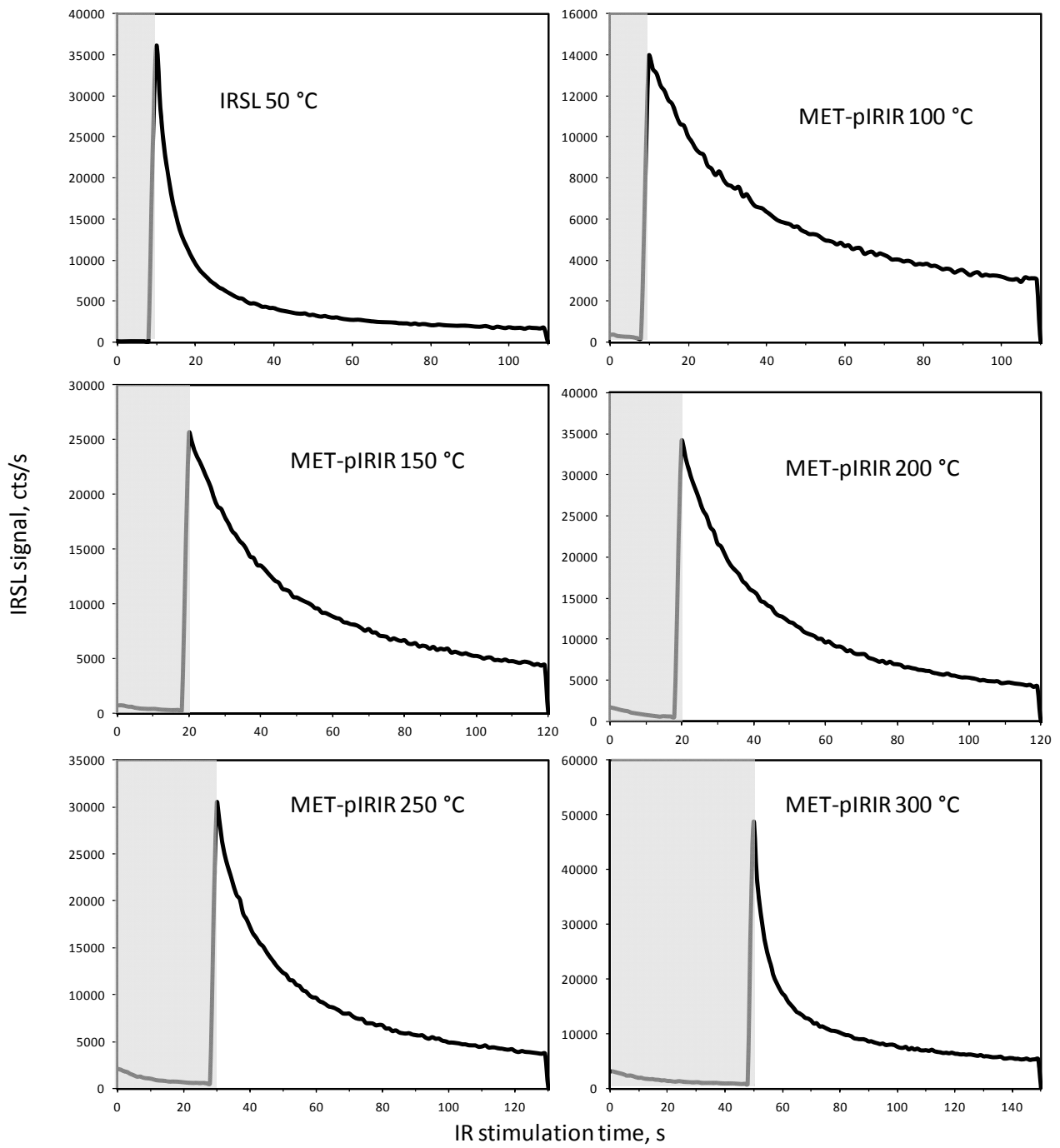
Figure 1
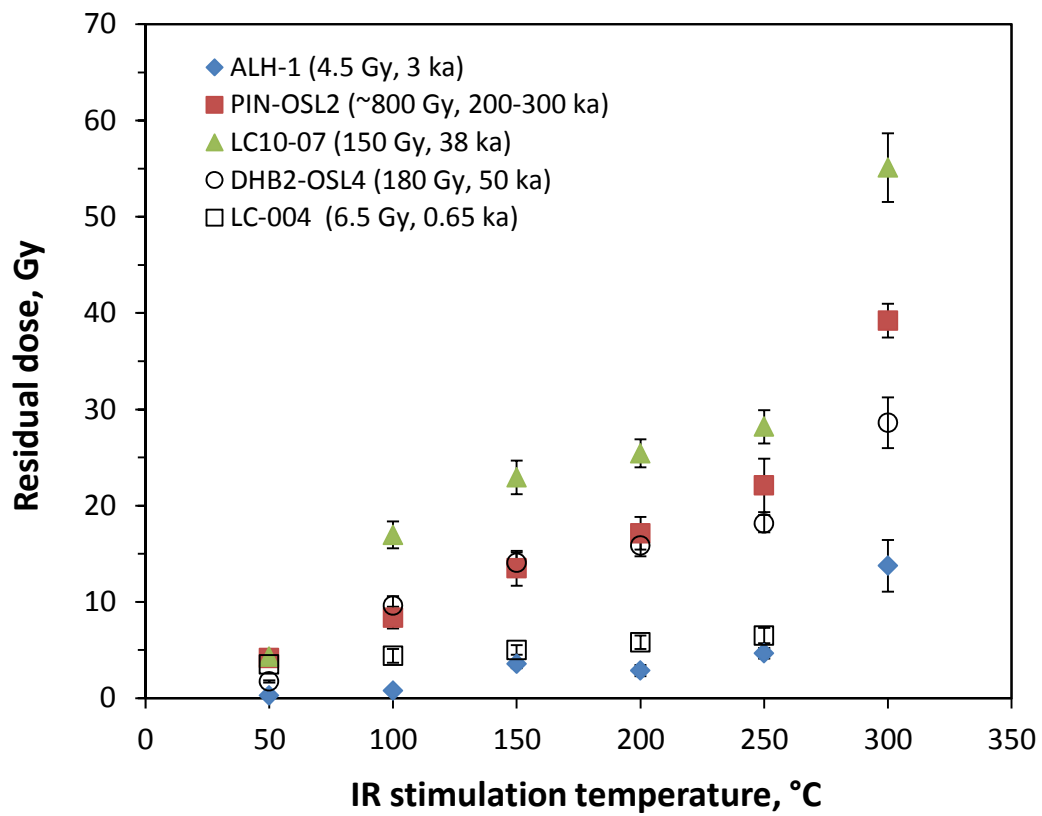
Figure 2
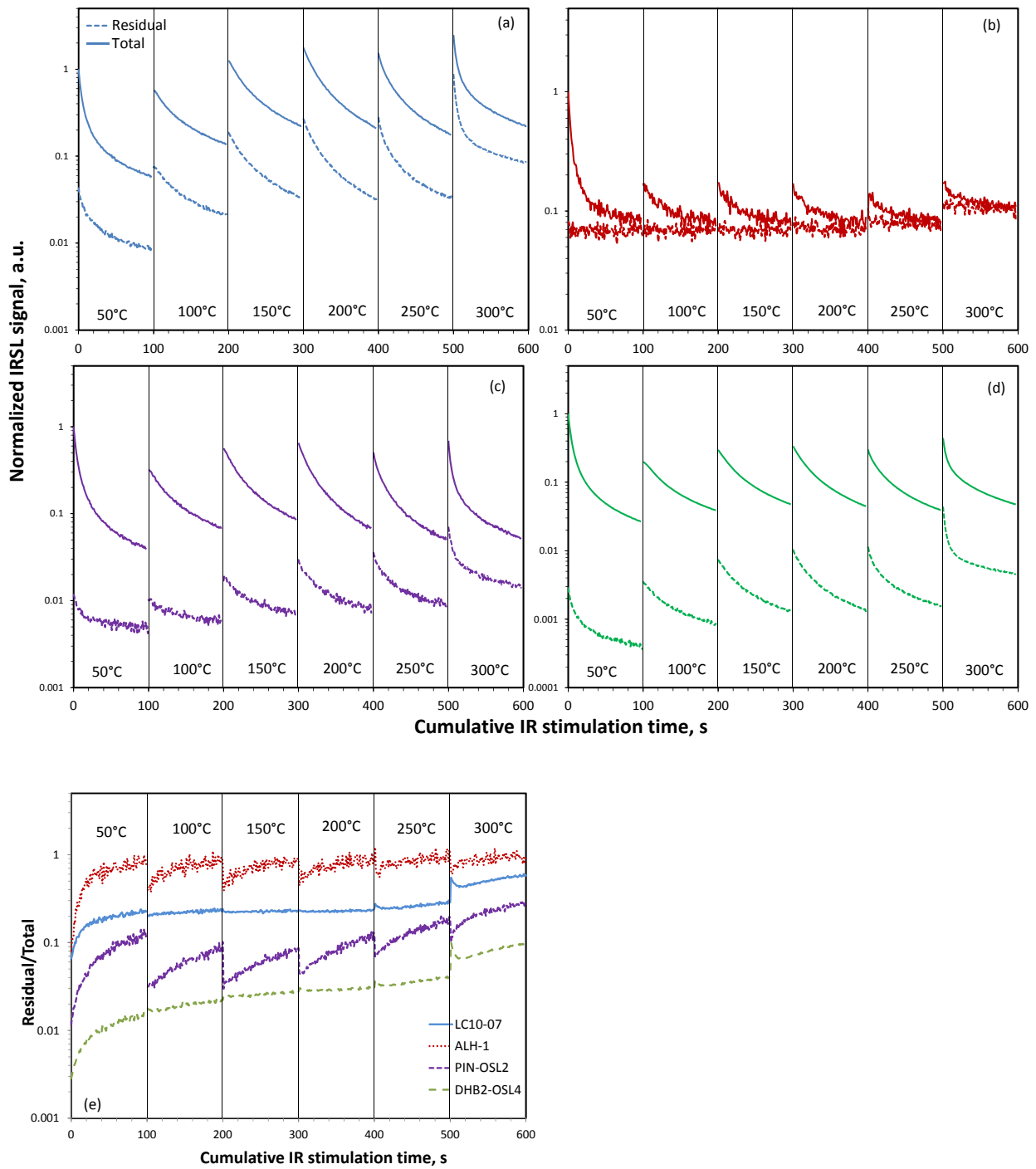
Figure 3
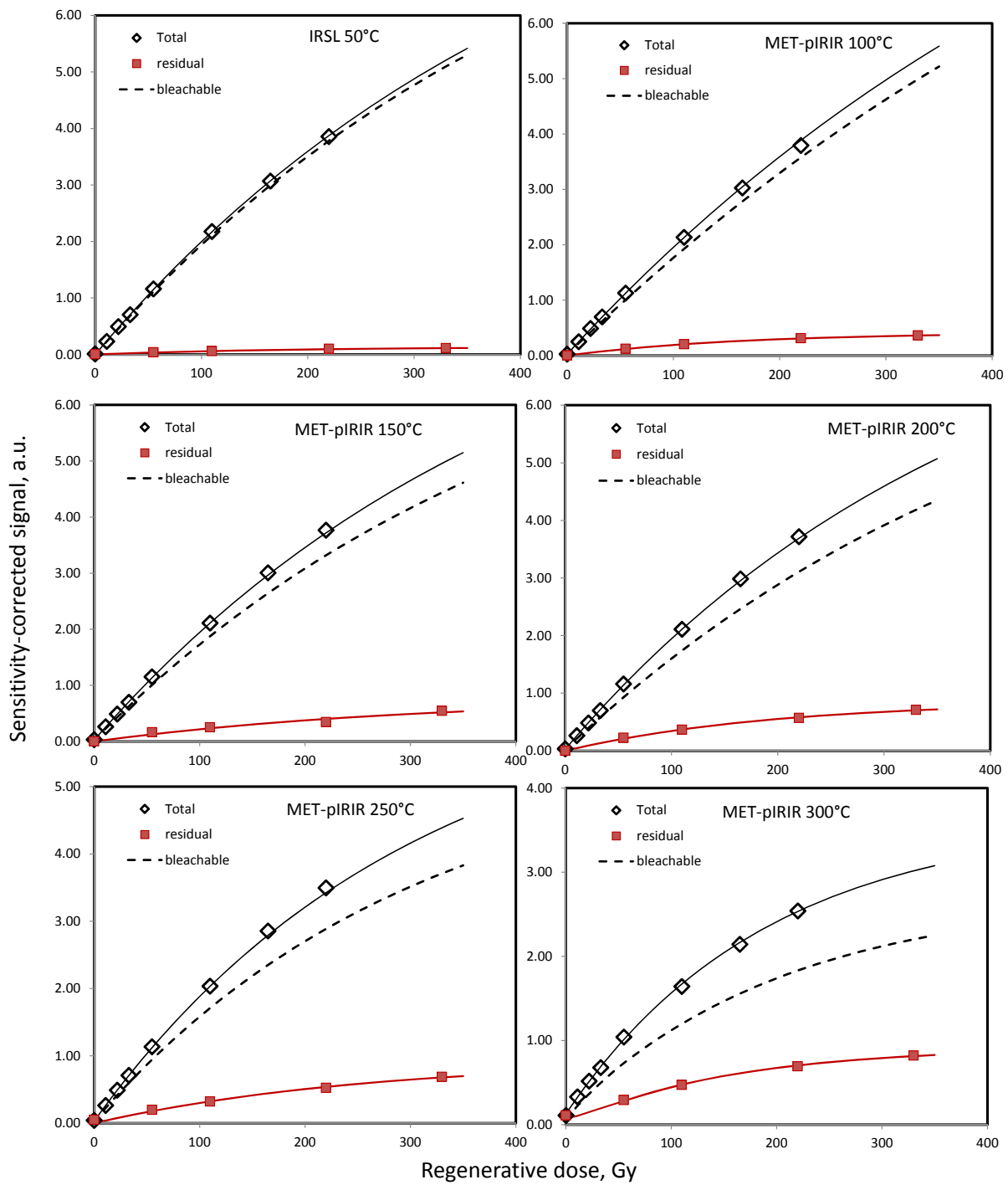
Figure 4
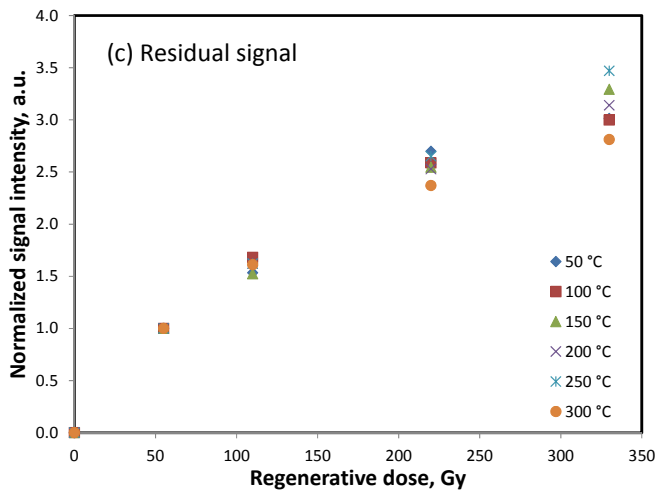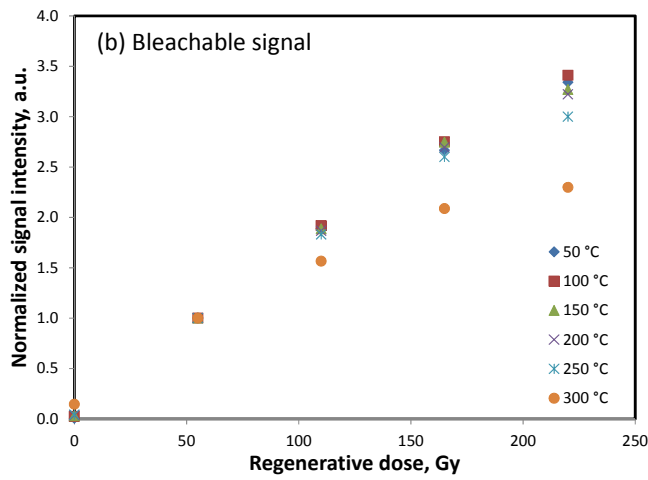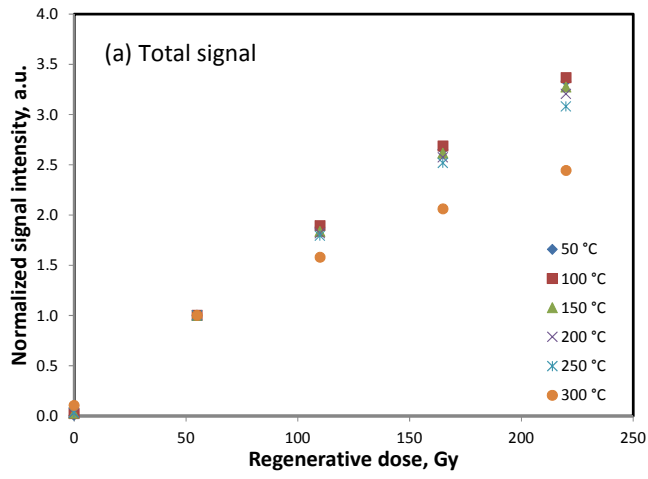
Figure 5
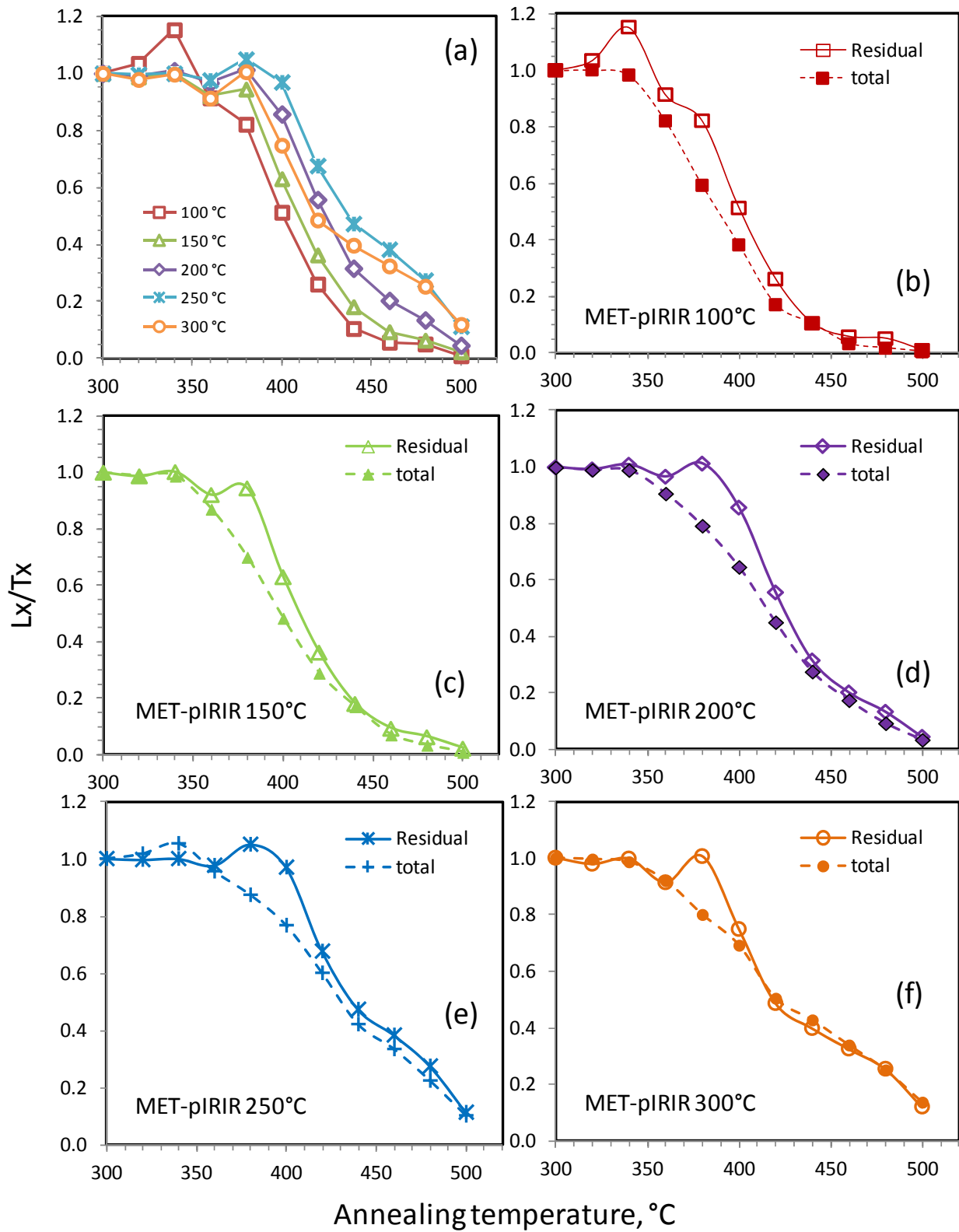
Figure 6
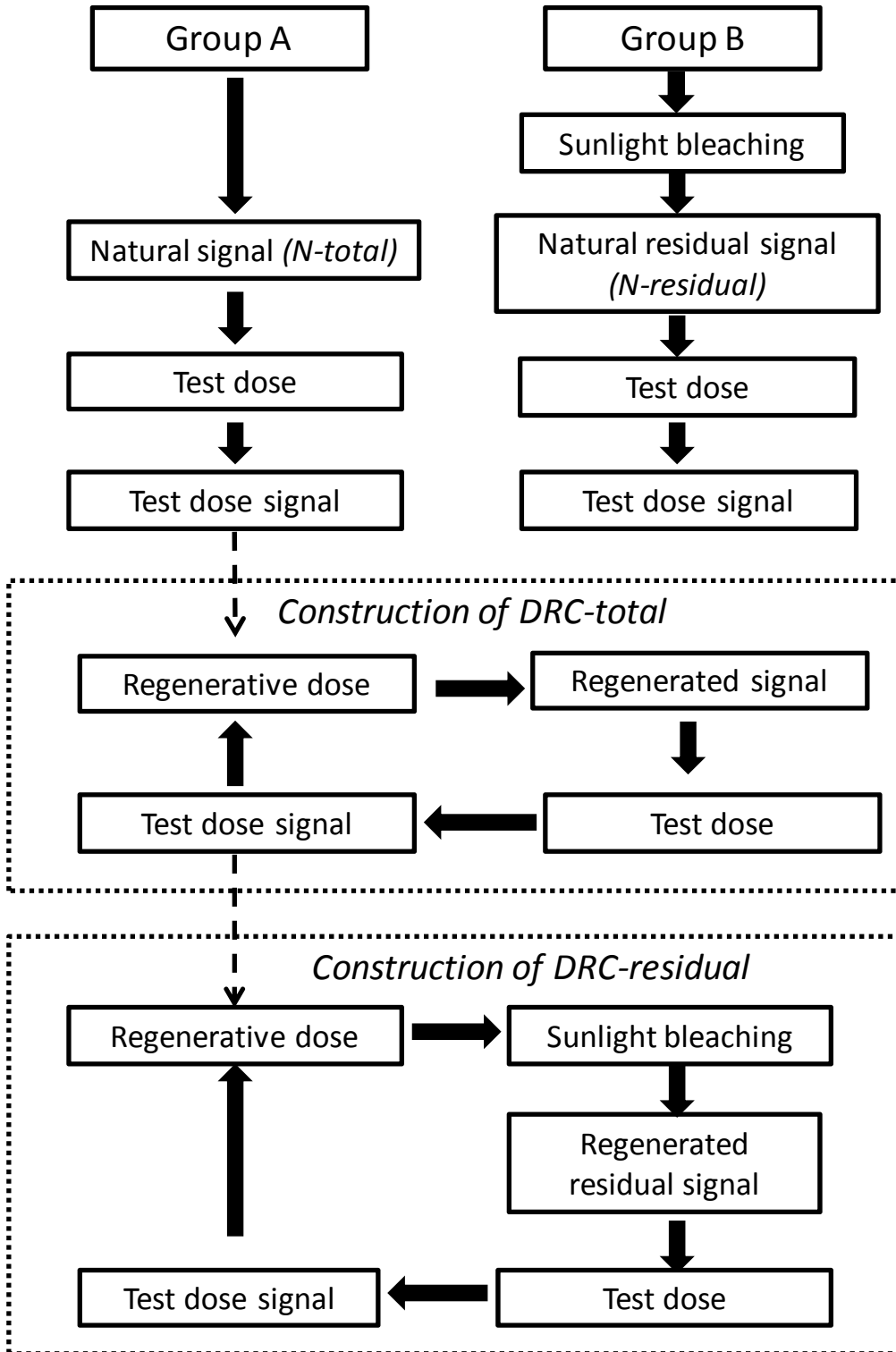
Figure 7
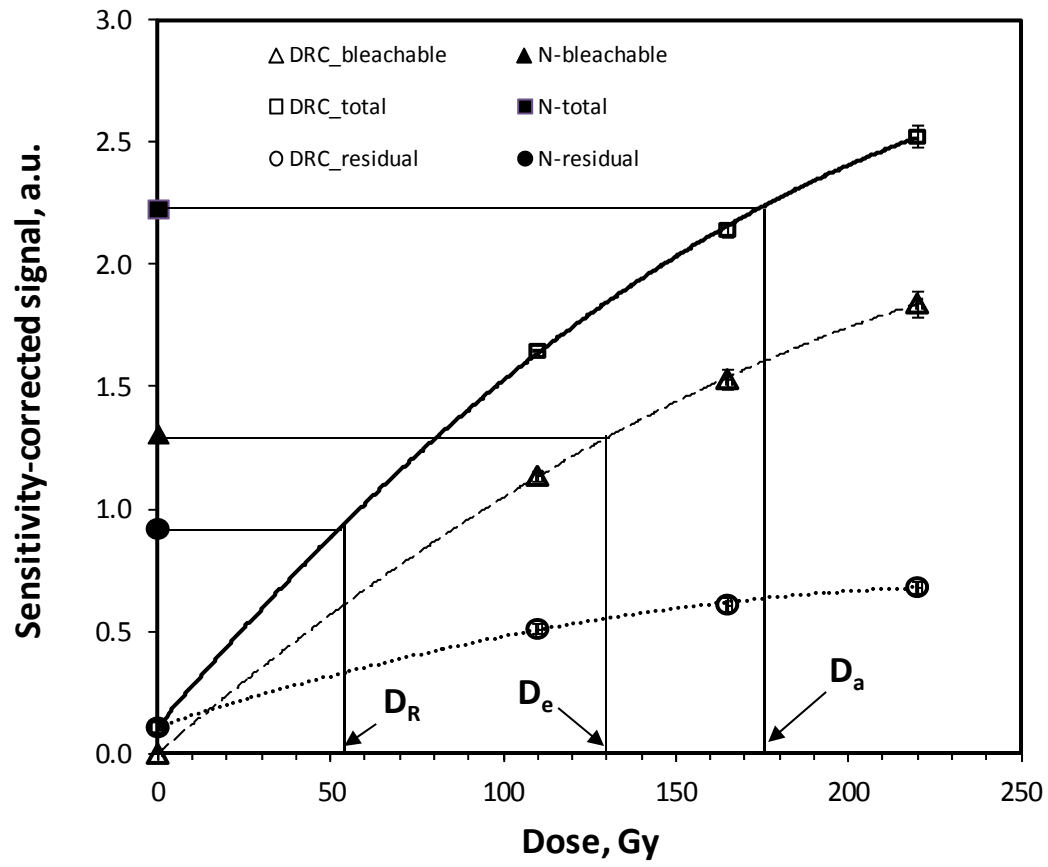
Figure 8
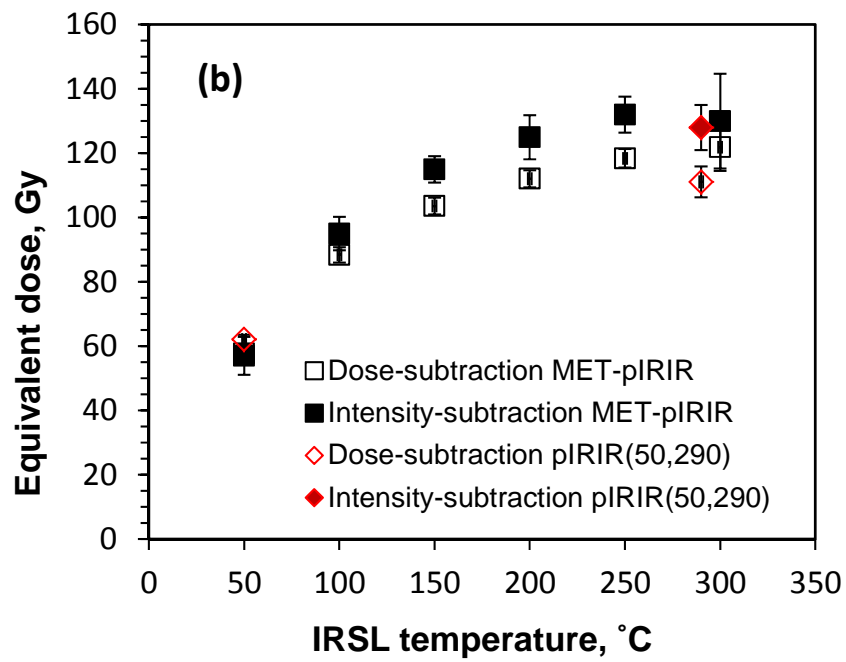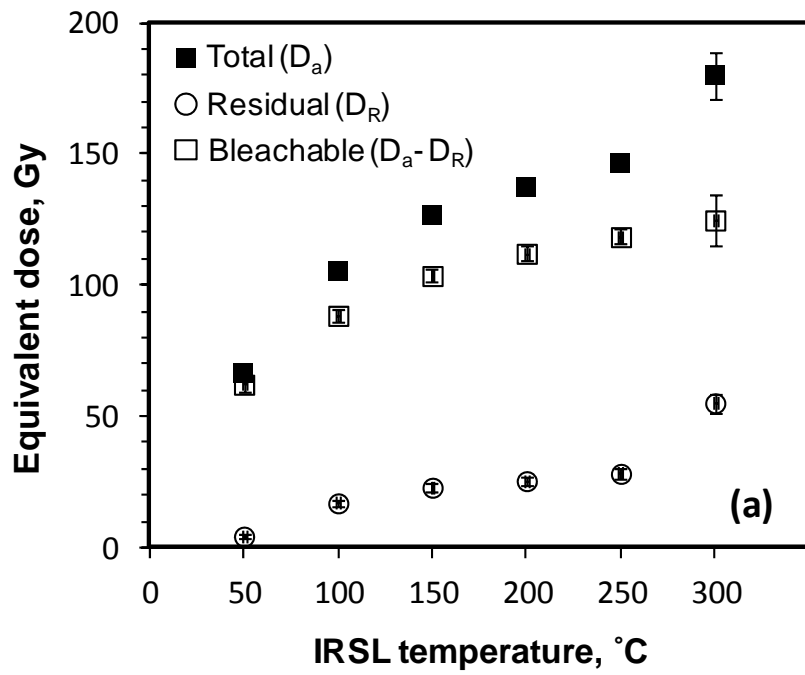
Figure 9
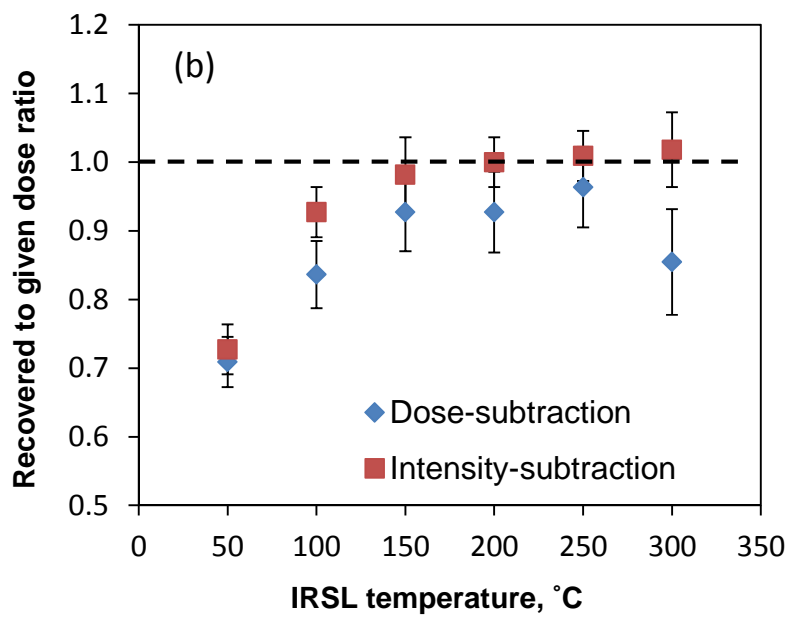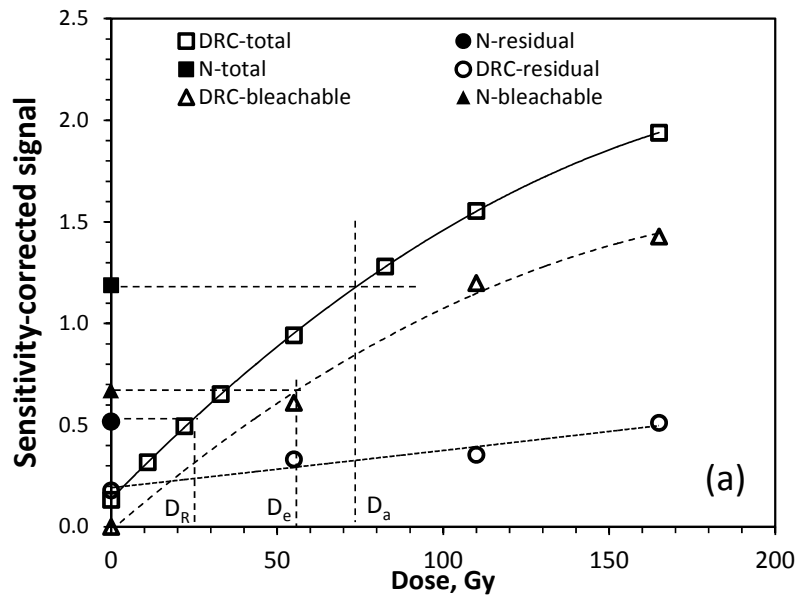
Figure 10

Table 1: Sample locations, grain size fractions used for experiments, expected ages and equivalent doses.

Sample code	Country of origin	Grain size used (µm)	Approximate expected depositional age (ka)	Measured or expected equivalent dose (Gy) [a]
LC-004	China	63–90	0.65	6.5 ± 0.7
ALH-1	Oman	90–125	3	4.5
LC10-07	France	90–125	38	147 ± 28
DHB2-OSL4	India	125–180	50	183 ± 18
PIN-OSL2	Georgia	90–125	200-300	700-900

[a] The equivalent dose of sample PIN-OSL2 is based on the expected depositional age multiplied by the measured environmental dose rate, while the value shown for sample ALH-1 represents the measured OSL equivalent dose for 90–125 µm grains of quartz with an adjustment for the larger internal dose rate to K-feldspar grains. The equivalent doses for other 3 samples are estimated from the MET-pIRIR(250°C) signal without any residual dose correction.

Table 2: Single-aliquot regenerative-dose (SAR) procedure used for multiple elevated temperature post-IR IRSL (MET-pIRIR) measurements.

MET-pIRIR protocol		
Step	Treatment	Observed
1	Give regenerative dose, D_i [a]	
2	Preheat at 320°C for 60 s	
3	[b] IRSL measurement at 50°C for 100 s	L_x
4	[b] IRSL measurement at 100°C for 100 s	$L_{x(100)}$
5	[b] IRSL measurement at 150°C for 100 s	$L_{x(150)}$
6	[b] IRSL measurement at 200°C for 100 s	$L_{x(200)}$
7	[b] IRSL measurement at 250°C for 100 s	$L_{x(250)}$
8	[b] IRSL measurement at 300°C for 100 s	$L_{x(300)}$
9	Give test dose, D_t	
10	Preheat at 320°C for 60 s	
11	[b] IRSL measurement at 50°C for 100 s	$T_{x(50)}$
12	[b] IRSL measurement at 100°C for 100 s	$T_{x(100)}$
13	[b] IRSL measurement at 150°C for 100 s	$T_{x(150)}$
14	[b] IRSL measurement at 200°C for 100 s	$T_{x(200)}$
15	[b] IRSL measurement at 250°C for 100 s	$T_{x(250)}$
16	[b] IRSL measurement at 300°C for 100 s	$T_{x(300)}$
17	IR bleaching at 340°C for 100 s	
18	Return to step 1	

[a] For the 'natural' and sunlight-bleached samples, i= 0 and D_0 = 0. The whole sequence is repeated for several regenerative doses including a zero dose and a repeat dose.

[b] For each IRSL measurement, an 'IR-off' period was applied to minimise the isothermal decay signal (Fu et al., 2012). That is, the aliquots were held for 10, 10, 20, 20, 30 and 50 s at the stimulation temperatures of 50, 100, 150, 200, 250 and 300°C (steps 3–8 and 11–16), respectively, before switching on the IR diodes to measure the IRSL signal.

Table 3. Summary of the characteristic saturation doses of the dose response curves for various MET-pIRIR signals from sample LC10-07.

Signal	Characteristic saturation dose (D_0, in Gy) of MET-pIRIR signal at specified stimulation temperature					
	50°C	100°C	150°C	200°C	250°C	300°C
Total	450 ± 83	600 ± 80	420 ± 71	395 ± 86	301 ± 26	189 ± 17
Residual	184 ± 31	163 ± 6	210 ± 45	196 ± 16	207 ± 42	176 ± 25
Bleachable	423 ± 28	453 ± 73	350 ± 109	352 ± 96	257 ± 65	157 ± 25